Supporting Information

for

pH-Responsive Multifunctional Theranostic Rapamycin-loaded Nanoparticles for Imaging and Treatment of Acute Ischemic Stroke

Yan Cheng[1], Airong Cheng[2], Yanlong Jia[3], Lin Yang[1], Yan Ning[4], Liang Xu[1], Yazhi Zhong[1], Zerui Zhuang[5], Jitian Guan[1], Xiaolei Zhang[1], Yan Lin[1], Teng Zhou[6], Xiusong Fan[7], Jianwu Li[8], Peng Liu[9], Gen Yan[10*], Renhua Wu[1*]*

[1] Department of Radiology, the Second Affiliated Hospital, Shantou University Medical College, Shantou 515041, Guangdong, China.

[2] Department of Neurology, Chengwu County People's Hospital, Chengwu 274200, Shandong, China.

[3] Department of Radiology, Xiangyang Central Hospital, Affiliated Hospital of Hubei University of Arts and Science, Hubei 441021, China.

[4] Shenzhen Maternity & Child Healthcare Hospital Affiliated to Southern Medical University, Shenzhen 518028, Guangdong, China.

[5] Department of Neurosurgery, Sun Yat-Sen Memorial Hospital, Sun Yat-Sen University, Guangzhou 510120, China; Department of Neurosurgery, Shantou Central Hospital, Affiliated Shantou Hospital of Sun Yat-sen University, Shantou 515041, Guangdong, China; Department of Neurosurgery, Second Affiliated Hospital, Shantou University Medical College, Shantou 515041, Guangdong, China.

[6] Department of Computer Science, Shantou University, Shantou 515041, China.

[7] Department of Radiology, Peking University Shenzhen Hospital, Shenzhen 518036, Guangdong, China.

[8] Transfusion Department, Peking University Shenzhen Hospital, Shenzhen 518036, Guangdong, China.

[9] National & Local Joint Engineering Research Center of Orthopaedic Biomaterials, Department of Bone & Joint Surgery, Peking University Shenzhen Hospital, Shenzhen 518036, Guangdong, China.

[10] Department of Radiology, The Second Affiliated Hospital of Xiamen Medical College, Xiamen 361023, Fujian, China.

***Corresponding Author:**

Peng Liu, liupeng_polymer@126.com

Gen Yan, gyan@stu.edu.cn

Renhua Wu, rhwu@stu.edu.cn

Animal model of transient middle cerebral artery occlusion (tMCAO)

Focal cerebral ischemia was induced by intraluminal occlusion of the right middle cerebral artery (MCA) for 120 min. The rats were anesthetized by injecting 10% chloral hydrate intraperitoneally at a dose of 0.3 mL/100 g under spontaneous breathing conditions. The monofilament was inserted into the internal carotid artery through the external carotid artery until it reached the MCA, at approximately 18 mm, causing cerebral ischemia. The thread was maintained intravascular for 2 h before permitting perfusion. In the sham group, MCA was not occluded, but the right common carotid arteries were peeled. Notably, model animals were kept alone until they were awake.

Evaluation of neurological deficit

Zea-Longa

Briefly, a score of 0 indicated no visible neurological deficits. Score 1 indicated mild neurological disorders, such as dysfunction in stretching contralateral forelimb and forepaw; score 2 indicated that animals showed circling behavior while walking; score 3 was assigned to animals that fell to the opposite side of cerebral ischemia while walking; score 4 was assigned to animals with a walking disorder accompanied by altered levels of consciousness, and score 5 indicated death.

Forelimb placement test induced by tentacles

This experiment was used to evaluate the self-sensory ability and sensorimotor function in animals. In brief, after tentacle stimulation, healthy rats quickly put their ipsilateral forelimb on the corner edge of a table, whereas the rats with cerebral ischemia could not complete this behavior because cerebral ischemia affected the contralateral forelimb response. The animals correctly placing the forelimb on the corner edge of the table scored 1 point. The number for which each rat correctly placed its left forelimb during ten experiments was recorded.

Foot fault test

Sensorimotor coordination of the forelimbs was assessed by the foot fault test. Rats were placed in an elevated stainless steel standard cage and allowed to explore the frame for 1 min and were given three trials. When the animals placed the forelimb incorrectly on the frame, and the forepaw fell through or slipped between the wires, it was counted as a fault. The percentage of foot faults of the left forepaw with respect to the total fault steps was calculated.

***In vivo* toxicity assessment**

We further evaluated the biocompatibility of the nanoparticles in vivo by using healthy C57BL mice (n=12) with an average weight of 30 g. Mice were divided into three groups; one group was injected with saline, and the two other groups were injected with NPs and Gd^{3+}@NPs respectively at a dose of 10 mg/Kg once via the tail vein. Then the mice were weighed daily and observed for mental and behavioral status for 7 days. On day 7, major organs were extracted and fixed in paraformaldehyde for HE staining to observe histological changes between the three groups.

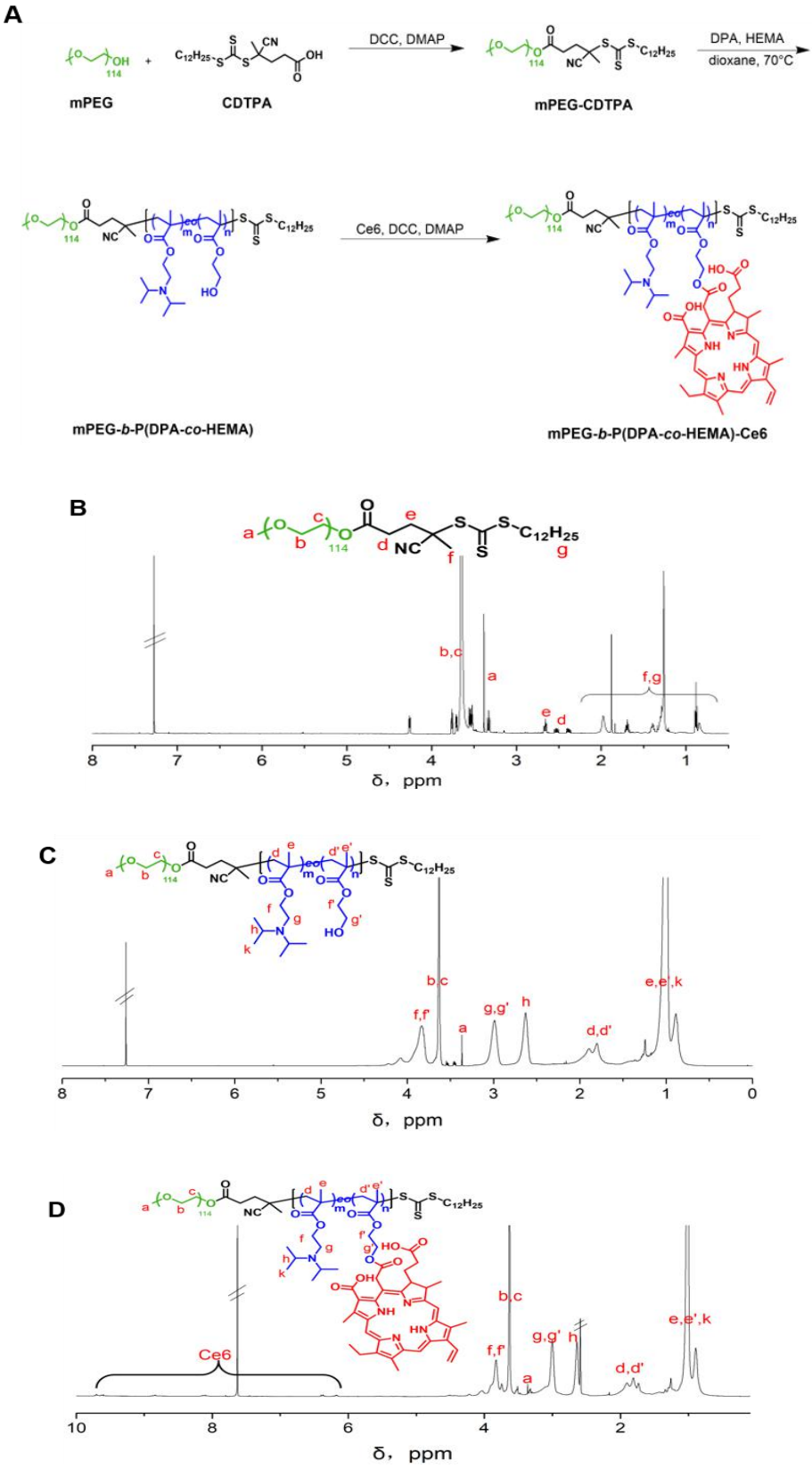

Figure. S1 Preparation and characterization of mPEG-*b*-P(DPA-*co*-HEMA)-Ce6. (A) Synthetic route of mPEG-*b*-P(DPA-*co*-HEMA)-Ce6. (B, C, D) ^{1}H-NMR spectra of mPEG-CDTPA, mPEG-*b*-P(DPA-*co*-HEMA) and mPEG-*b*-P(DPA-*co*-HEMA)-Ce6.

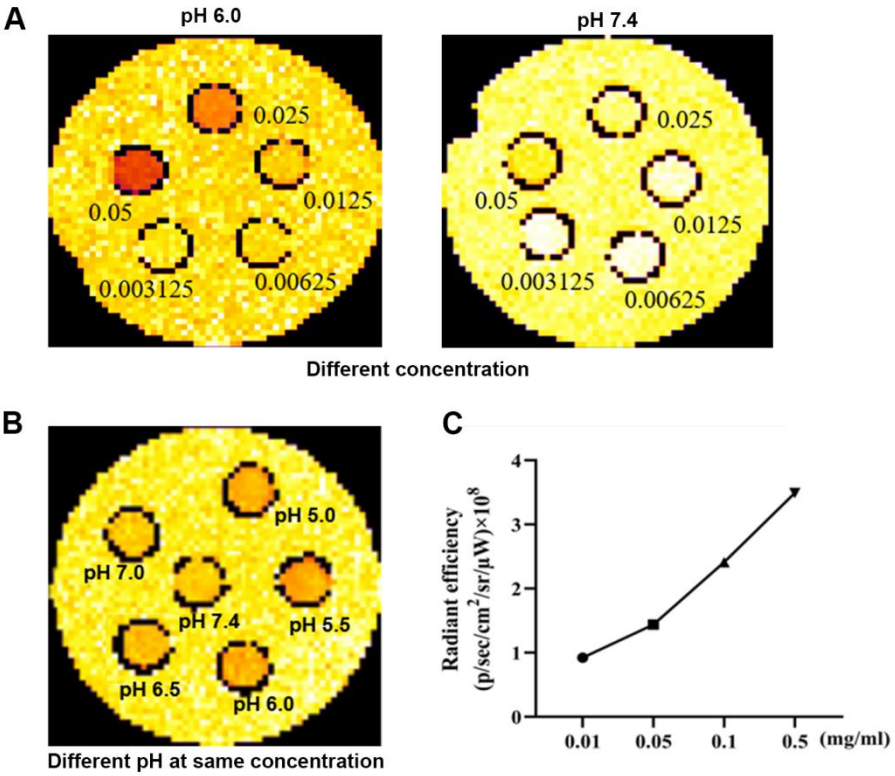

Figure. S2 The properties of MR and NIF imaging of multifunctional nanoparticles that can be controlled with acidic stimuli: (A) The T1 mapping images at different Gd^{3+} concentrations (mM) at pH 6.0 and pH 7.4. (B) The T1 mapping images at different pH values (0.5 mg/mL). (C) Fluorescence property of different concentrations of nanoparticles at pH 6.0.

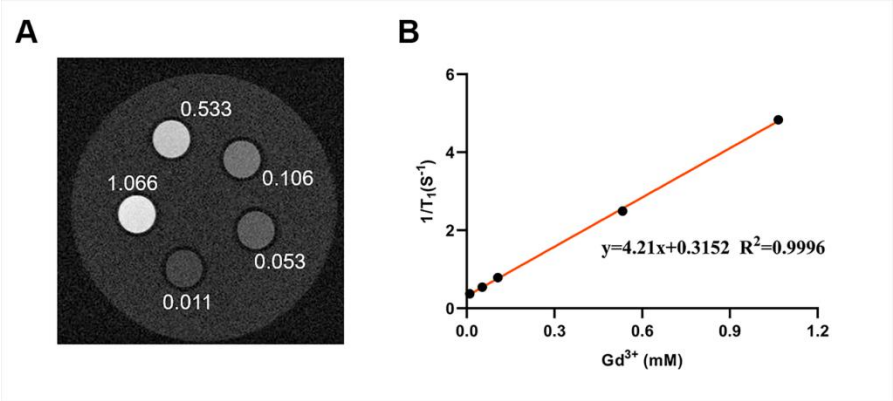

Figure. S3 T1-weighted MR properties of the Gd-DTPA at different Gd^{3+} concentrations (mM) (Magnevist, contrast agent commonly used in clinical practice). (A) T1-weighted MR images of the Magnevist. (B) Plots of 1/T1 as a function of Gd^{3+} concentration.

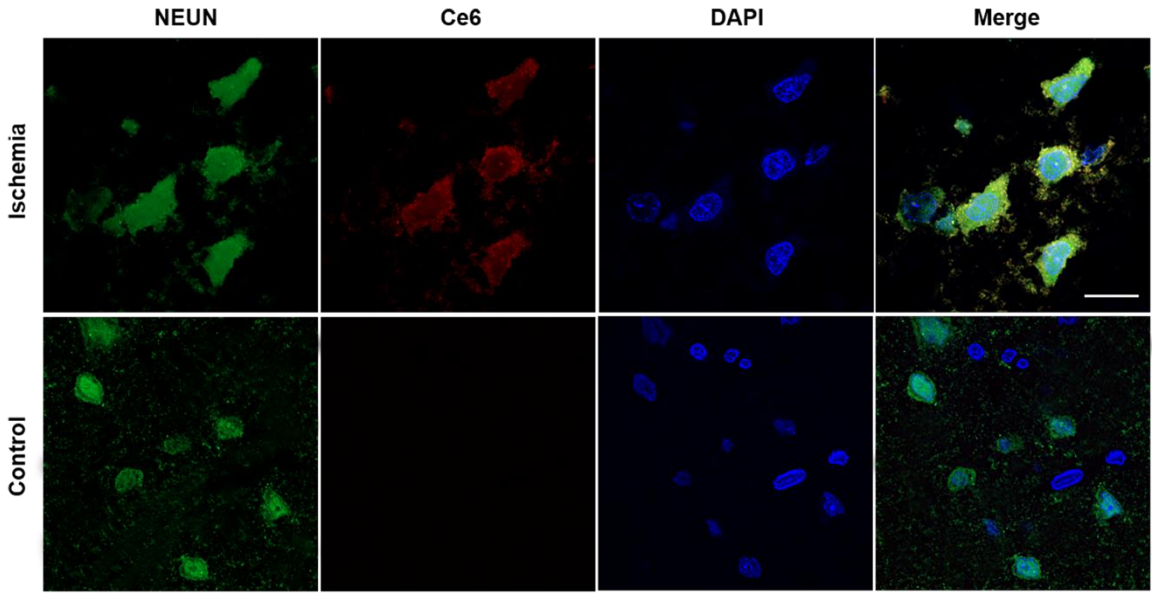

Figure. S4 CLSM images of the brain tissue sections showed that nanoparticles were efficiently internalized by neuronal cells (NEUN: neuronal staining (green); Ce6: nanoparticles (red); scale bar = 20 μm).

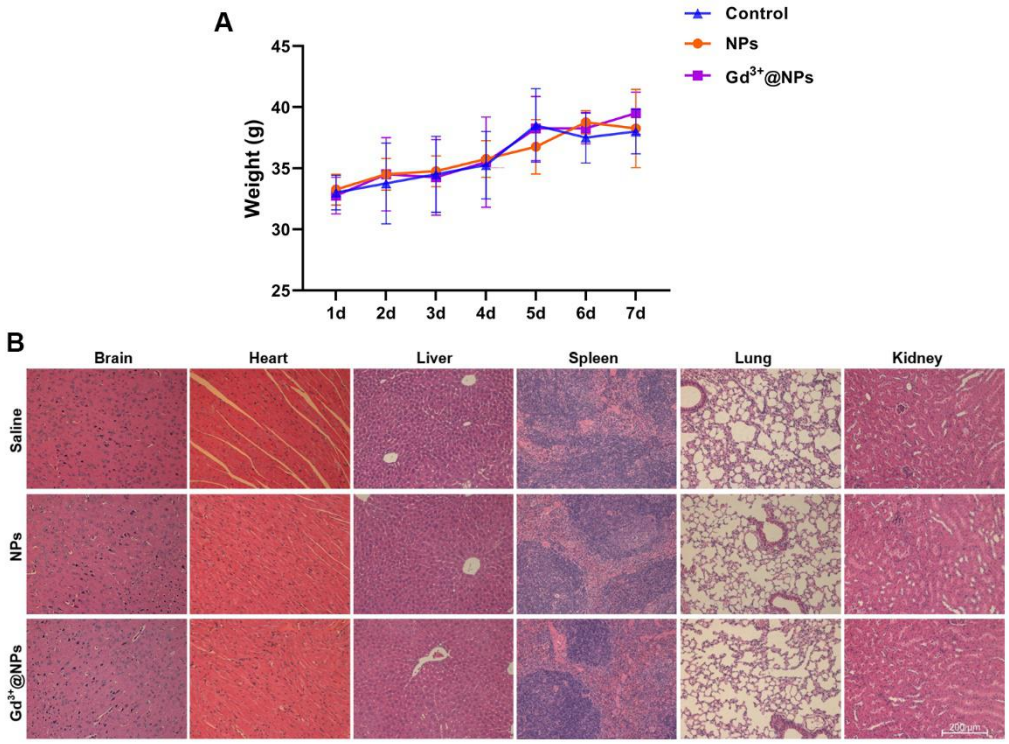

Figure. S5 The biocompatibility of nanoparticles *in vivo*. (A) The body weight change of the mice was measured daily. (B) H&E staining of the sections of major tissues (scale bar = 200 μm).

Table S1. **Comparison of the r1 values of MRI positive contrast agents used in clinical practice**

Short Name	**Generic name**	**r1 ($mM^{-1}s^{-1}$)**	**references**
Gd-DOTA	Gadoterate meglumine	2.72-4.2	2, 3, 4, 5
Gd-HP-DO3A	Gadoteridol	2.61-4.4	1, 2, 3, 4, 5
Gd-DTPA	Gadopentate dimeglumine	3.1-5.1	3, 4, 6, 7, 8
Gd-DTPA-BMEA	Gadoversetamide	3.6-5.2	2, 3, 4
Gd-DTPA-BMA	Gadodiamide	3.2-4.1	1, 2, 4
Gd-BOPTA	Gadobenate dimeglumine	4.0-5.0	2, 3, 4
Gd-EOB-DTPA	Gadoxetic acid	4.3-6.3	2, 3, 4
Ms-325	Gadofosveset trisodium	5.2-6.9	2, 3
Gd-DO3A-butrol	Gadobutrol	3.83-5.3	2, 3, 4, 5
Gd^{3+}@NPs (**this study**)		11.01±1.03	

REFERENCES

(1) Chang, C. A. Magnetic Resonance Imaging Contrast Agents. Design and Physicochemical Properties of Gadodiamide. *Invest Radiol.* **1993**, *28*, S21-7. DOI: 10.1097/00004424-199303001-00003.

(2) Rohrer, M.; Bauer, H.; Mintorovitch, J.; Requardt, M.; Weinmann, H. J. Comparison of Magnetic Properties of MRI Contrast Media Solutions at Different Magnetic Field Strengths. *Invest Radiol.* **2005**, *40* (11), 715-24. DOI: 10.1097/01.rli.0000184756.66360.d3.

(3) Noebauer-Huhmann, I. M.; Szomolanyi, P.; Juras, V.; Kraff, O.; Ladd, M. E.; Trattnig, S. Gadolinium-Based Magnetic Resonance Contrast Agents at 7 Tesla: in Vitro T1 Relaxivities in Human Blood Plasma. *Invest Radiol*. **2010**, *45* (9), 554-8. DOI: 10.1097/RLI.0b013e3181ebd4e3.

(4) Shen, Y.; Goerner, F. L.; Snyder, C.; Morelli, J. N.; Hao, D.; Hu, D.; Li, X.; Runge, V. M. T1 Relaxivities of Gadolinium-Based Magnetic Resonance Contrast Agents in Human Whole Blood at 1.5, 3, and 7 T. *Invest Radio*l. **2015**, *50* (5), 330-8. DOI: 10.1097/RLI.0000000000000132.

(5) Szomolanyi, P.; Rohrer, M.; Frenzel, T.; Noebauer-Huhmann, I. M.; Jost. G.; Endrikat. J.; Trattnig. S.; Pietsch. H. Comparison of the Relaxivities of Macrocyclic Gadolinium-Based Contrast Agents in Human Plasma at 1.5, 3, and 7 T, and Blood at 3 T. *Invest Radiol*. **2019**, *54* (9), 559-564. DOI: 10.1097/RLI.0000000000000577.

(6) Wang, T.; Wang, D.; Yu, H.; Wang, M.; Liu, J.; Feng, B.; Zhou, F.; Yin, Q.; Zhang, Z.; Huang, Y.; Li, Y. Intracellularly Acid-Switchable Multifunctional Micelles for Combinational Photo/Chemotherapy of the Drug-Resistant Tumor. *ACS Nano*. **2016**, *10* (3), 3496-508. DOI: 10.1021/acsnano.5b07706.

(7) Wang, Y.; Yang, T.; Ke, H.; Zhu, A.; Wang, Y.; Wang, J.; Shen, J.; Liu, G.; Chen, C.; Zhao, Y.; Chen, H. Smart Albumin-Biomineralized Nanocomposites for Multimodal Imaging and Photothermal Tumor Ablation. *Adv Mater*. **2015**, *27* (26), 3874-82. DOI: 10.1002/adma.201500229.

(8) Hou, W.; Jiang, Y.; Xie, G.; Zhao, L.; Zhao, F.; Zhang, X.; Sun, S. K.; Yu, C.; Pan, J. Biocompatible BSA-Mno_2 Nanoparticles for *in Vivo* Timely Permeability Imaging of Blood-Brain Barrier and Prediction of Hemorrhage Transformation in Acute Ischemic Stroke. *Nanoscale*. **2021**, *13* (18), 8531-8542. DOI: 10.1039/d1nr02015c.